# Raman spectroscopy of the multi-anion mineral mallestigite $Pb_3Sb^{5+}(SO_4)(AsO_4)(OH)_6 \cdot 3H_2O$ – a mineral of archaeological significance

**Ray L. Frost, • Sara J. Palmer, Yunfei Xi and Keqin Tan**

Chemistry Discipline, Faculty of Science and Technology, Queensland University of Technology, GPO Box 2434, Brisbane Queensland 4001, Australia.

## Abstract

Some minerals are formed which show poorly defined X-ray diffraction patterns. Vibrational spectroscopy offers one of the few methods for the assessment of the structure of the oxyanions in such minerals. Among this group of minerals is mallestigite with formula $Pb_3Sb^{5+}(SO_4)(AsO_4)(OH)_6 \cdot 3H_2O$. The objective of this research is to determine the molecular structure of the mineral mallestigite using vibrational spectroscopy. Raman and infrared bands are attributed to the $AsO_4^{3-}$ , $SO_4^{2-}$ and water stretching vibrations. Mallestigite is a mineral formed in ancient waste dumps such as occurs at Mallestiger, Carinthia, Austria and as such is a mineral of archaeological significance.

**Keywords:** Raman spectroscopy, mallestigite, arsenate, sulphate, archaeology

• Author to whom correspondence should be addressed (r.frost@qut.edu.au)

## Introduction

The mineral mallestigite $Pb_3Sb(SO_4)(AsO_4)(OH)_6 \bullet 3H_2O$ is a multi-anion mineral of lead and antimony [1]. The mineral is monoclinic of point group 2/*m* and space group *C*2/*m* [2]. Crystals are tabular or prismatic, elongated along [001] [2]. Mallestigite belongs to the fleischerite mineral group. Mallestigite is a rare secondary mineral in the oxidized zone of a hydrothermal polymetallic base-metal deposit as may be found at Tiger, Arizona, USA. The mineral is found in the slag dumps of Laurium, Greece [3-5]. The mineral is of archaeological significance. It is formed as a reaction product of mine wastes and sea water. Old mine sites from ancient Greece contain oxides of lead and antimony. The mineral acts as an arsenate and sulphate accumulator.

The reason for this research is that minerals such as mallestigite are found in soils and in old mine sites. Therefore, this research focuses on the spectroscopic determination of mallestigite and consequential molecular structure. Raman spectroscopy has proven very useful for the study of minerals [6-13]. Indeed Raman spectroscopy has proven most useful for the study of diagenetically related minerals as often occurs with minerals containing arsenate and sulphate groups, including pitticite and zykaite. Raman spectroscopy is especially useful when the minerals are X-ray non-diffracting or poorly diffracting and very useful for the study of amorphous and colloidal minerals [14-23]. Mallestigite is a mineral which falls into this category. This paper is a part of systematic studies of vibrational spectra of minerals of secondary origin in the oxide supergene zone. In this work we attribute bands at various wavenumbers to vibrational modes of mallestigite using Raman spectroscopy and relate the spectra to the structure of the mineral.

# Experimental

## Minerals

The mineral mallestigite was supplied by the Mineralogical research Company. The mineral sample originated from a waste dump from a copper-lead-zinc mine, 1 km north west of Mallestiger, Carinthia, Austria, Details of the mineral have been published [24]. The

mineral is found in the slag deposits of Laurium, Greece and is formed by the reaction of slag with sea water [3].

## Raman spectroscopy

Crystals of mallestigite were placed on a polished metal surface on the stage of an Olympus BHSM microscope, which is equipped with 10x, 20x, and 50x objectives. The microscope is part of a Renishaw 1000 Raman microscope system, which also includes a monochromator, a filter system and a CCD detector (1024 pixels). The Raman spectra were excited by a Spectra-Physics model 127 He-Ne laser producing highly polarised light at 633 nm and collected at a nominal resolution of 2 $cm^{-1}$ and a precision of ± 1 $cm^{-1}$ in the range between 100 and 4000 $cm^{-1}$. Repeated acquisition on the crystals using the highest magnification (50x) was accumulated to improve the signal to noise ratio in the spectra. Spectra were calibrated using the 520.5 $cm^{-1}$ line of a silicon wafer.

## Infrared spectroscopy

Infrared spectra were obtained using a Nicolet Nexus 870 FTIR spectrometer with a smart endurance single bounce diamond ATR cell. Spectra over the 4000–525 $cm^{-1}$ range were obtained by the co-addition of 64 scans with a resolution of 4 $cm^{-1}$ and a mirror velocity of 0.6329 cm/s. Spectra were co-added to improve the signal to noise ratio.

Band component analysis was undertaken using the Jandel 'Peakfit' (Erkrath, Germany) software package which enabled the type of fitting function to be selected and allowed specific parameters to be fixed or varied accordingly. Band fitting was done using a Lorentz-Gauss cross-product function with the minimum number of component bands used for the fitting process. The Lorentz-Gauss ratio was maintained at values greater than 0.7 and fitting was undertaken until reproducible results were obtained with squared correlations ( $r^2$) greater than 0.995. Band fitting of the spectra is quite reliable providing there is some band separation or changes in the spectral profile.

## Results and discussion

### Background

S.D. Ross in Farmer's treatise [25] reported the infrared spectrum of beudantite (Table 18.IX page 433). This table compares the infrared spectra of minerals from the alunite-jarosite supergroups. Ross reported infrared bands at 985, 1006 $cm^{-1}$ ($\nu_1$), 430, 466 $cm^{-1}$ ($\nu_2$), 1078,

1160 $cm^{-1}$ ($\nu_3$), 600, 625 and 670 $cm^{-1}$ ($\nu_4$). OH vibrations were reported at 3420 and 525 $cm^{-1}$ attributed to the stretching and bending of the OH units. The sulphate stretching mode for Cu-beudantite [26] was listed as 1010 $cm^{-1}$ and the $\nu_2$ bending modes were reported at 620, 662 and 687 $cm^{-1}$. The arsenate stretching bands were listed as occurring at 729, 813, 821, 851 and 870 $cm^{-1}$. The arsenate bending modes were not reported, no doubt because these bands occurred outside the detection limits of the instrument.

The $T_d$ symmetry is characteristic for both free units $(SO_4)^{2-}$ and $(AsO_4)^{3-}$ ions. In dilute aqueous solutions, $(SO_4)^{2-}$ ions exhibit the symmetric stretching vibration ($A_1$, $\nu_1$), 983 $cm^{-1}$ – Raman active, the doubly degenerate bending vibration ($E$, $\nu_2$), 450 $cm^{-1}$ – Raman active, the triply degenerate antisymmetric stretching vibration ($F_2$, $\nu_3$), 1105 $cm^{-1}$ – Raman and infrared active, and the triply degenerate bending vibration ($F_2$, $\nu_4$), 611 $cm^{-1}$ – Raman and infrared active. Any symmetry lowering may activate some or all vibrations in both Raman and IR and cause the splitting of degenerate vibrations [27-29] . Fundamental vibrational modes for $(AsO_4)^{3-}$ are the symmetric stretching vibration ($A_1$, $\nu_1$), 837 $cm^{-1}$ – Raman active, the doubly degenerate bending vibration ($E$, $\nu_2$), 349 $cm^{-1}$ – Raman active, the triply degenerate antisymmetric stretching vibration ($F_2$, $\nu_3$) – 878 $cm^{-1}$ – Raman and infrared active, and the triply degenerate bending vibration ($F_2$, $\nu_4$), 463 $cm^{-1}$ – Raman and infrared active. Similarly, as in the case of sulfate ions, any symmetry lowering may cause Raman and infrared activation of some or all vibrations and the splitting of degenerate vibrations [28, 30].

**Spectroscopy**

The Raman spectrum of mallestigite is displayed in the 100 to 1400 $cm^{-1}$ region in Figure 1. It should be noted that we were unable to collect the Raman spectrum in the OH stretching region, probably as a result of the disorder in the structure of the mineral. However the infrared spectrum of the OH stretching region was obtained. The complete infrared spectrum over the 500 to 4000 $cm^{-1}$ region is shown in Figure 2. The Raman spectrum of mallestigite in the 700 to 1400 $cm^{-1}$ region is displayed in Figure 3. The Infrared spectrum of mallestigite in the 500 to 1400 $cm^{-1}$ region is shown in Figure 4. An extremely intense band is observed at 978 $cm^{-1}$ and is assigned to the $SO_4^{2-}$ symmetric stretching mode. Low intensity bands are found at 803, 827 and 865 $cm^{-1}$. These bands are attributed to the $AsO_4^{3-}$ stretching modes. Low intensity Raman bands are found at 1062,

1151, 1158, 1234 and 1261 $cm^{-1}$. These bands are accounted for by the $SO_4^{2-}$ antisymmetric stretching modes.

The infrared spectrum shows considerable complexity. Infrared bands are observed at 778 and 798 $cm^{-1}$. These infrared bands are associated with the $AsO_4^{3-}$ stretching modes. Infrared bands are also observed at 993, 1035, 1089 and 1130 $cm^{-1}$. The band at 993 $cm^{-1}$ is the infrared equivalent of the Raman band at 978 $cm^{-1}$ attributed to the assigned to the $SO_4^{2-}$ symmetric stretching mode. The other infrared bands are attributed to the assigned to the $SO_4^{2-}$ antisymmetric stretching modes. The infrared band at 937 $cm^{-1}$ may be associated with a hydroxyl deformation mode.

The Raman spectrum of mallestigite in the 400 to 650 $cm^{-1}$ region is reported in Figure 5. This spectral region is where the $SO_4^{2-}$ and $AsO_4^{3-}$ bending modes are found. Raman bands are found at 606, 619, 631 and 641 $cm^{-1}$ and are assigned to the $\nu_4\ (SO_4)^{2-}$ bending modes. The two infrared bands at 688 and 694 $cm^{-1}$ may be the equivalent infrared bands (Figure 4). Four Raman bands are observed at 416, 437, 449 and 460 $cm^{-1}$. The Raman bands are attributable to the doubly degenerate $\nu_2\ (SO_4)^{2-}$ bending mode but may also overlap with the $AsO_4^{3-}$ bending modes (($F_2$, $\nu_4$)). Two Raman bands are observed at 340 and 354 $cm^{-1}$. These bands are assigned to the $AsO_4^{3-}$ ($E$, $\nu_2$) bending modes. Low wavenumber bands are shown in Figure 6. Strong bands are observed at 149, 157, 181 and 211 $cm^{-1}$. These bands are simply described as lattice modes.

The Raman spectrum of mallestigite in the OH stretching region displays a single intense broad band at 3336 $cm^{-1}$. The infrared spectrum shows a broad spectral profile of low intensity (Figure 7). Infrared bands may be resolved at 2984, 3066, 3287, 3491 and 3629 $cm^{-1}$. These bands are assigned to the water OH stretching vibrations. The infrared band at 3629 $cm^{-1}$ is due to the stretching vibration of OH units in the mallestigite structure.

## Conclusions

Mallestigite is an example of a mineral which resembles a gel and as such shows poorly defined X-ray diffraction patterns. The application of vibrational spectroscopy is of

importance as it offers one of the only methods for the assessment of the molecular structure of this mineral. Similar minerals are diadochite and dexterite.

The Raman spectrum of mallestigite is dominated by a very intense sharp band at 983 $cm^{-1}$ assigned to the $SO_4^{2-}$ symmetric stretching mode. The same vibrational mode is observed in the infrared spectrum as a sharp band at 978 $cm^{-1}$. Raman bands at 1062, 1151 and 1158 $cm^{-1}$ are observed and assigned to the $SO_4^{2-}$ antisymmetric stretching mode. The observation of multiple bands in the $\nu_4 (SO_4)^{2-}$ spectral region supports the concept of reduction in symmetry of the sulphate anion in the mallestigite structure. Raman bands observed at 432 and 465 $cm^{-1}$ are attributable to the doubly degenerate $\nu_2 (SO_4)^{2-}$ bending mode. Vibrational spectroscopy is important in the assessment of the molecular structure of the mallestigite, especially when the mineral is poorly-diffracting.

**Acknowledgments**

The financial and infra-structure support of the Queensland University of Technology, Chemistry discipline is gratefully acknowledged. The Australian Research Council (ARC) is thanked for funding the instrumentation.

## REFERENCES


[1] G. Schnorrer, Aufschluss 54 (2003) 42.

[2] H. Effenberger, TMPM, Tschermaks Miner. Petr. Mitt. 34 (1985) 279.

[3] R. Jaxel, P. Gelaude, Min. Rec. 17 (1986) 183.

[4] D.R. Peacor, P.J. Dunn, G. Schnorrer-Koehler, R.A. Bideaux, Min. Rec. 16 (1985) 117.

[5] C. Rewitzer, R. Hochleitner, Riv. Min. It. (1989) 83.

[6] R.L. Frost, E.C. Keeffe, S. Bahfenne, Spectrochim. Acta, A75 (2010) 1476.

[7] R.L. Frost, B.J. Reddy, E.C. Keeffe, Spectrochim. Acta, A77 (2010) 388.

[8] R.L. Frost, Spectrochim.Acta, 71A (2009) 1788.

[9] R.L. Frost, Spectrochim.Acta, A72 (2009) 903.

[10] R.L. Frost, S. Bahfenne, J. Graham, Spectrochimica Acta, Part A: Molecular and Biomolecular Spectroscopy 71A (2009) 1610.

[11] R.L. Frost, J. Cejka, Spectrochim.Acta, A71 (2009) 1959.

[12] R.L. Frost, J. Cejka, M.J. Dickfos, Spectrochim.Acta, A71 (2009) 1799.

[13] R.L. Frost, B.J. Reddy, S. Bahfenne, J. Graham, Spectrochim.Acta, A72 (2009) 597.

[14] R.L. Frost, J. Cejka, J. Sejkora, J. Plasil, B.J. Reddy, E.C. Keeffe, Spectrochim.Acta, A78 (2011) 494.

[15] R.L. Frost, S.J. Palmer, Spectrochim. Acta, A78 (2011) 248.

[16] R.L. Frost, S.J. Palmer, Spectrochim. Acta, A78 (2011) 1255.

[17] R.L. Frost, S.J. Palmer, Spectrochim. Acta, A78 (2011) 1250.

[18] R.L. Frost, S.J. Palmer, Spectrochim. Acta, A79 (2011) 1794.

[19] R.L. Frost, S.J. Palmer, Spectrochim. Acta, A79 (2011) 1215.

[20] R.L. Frost, S.J. Palmer, Spectrochim. Acta, A79 (2011) 1210.

[21] R.L. Frost, S.J. Palmer, S. Bahfenne, Spectrochim. Acta, A78 (2011) 1302.

184 [22] R.L. Frost, S.J. Palmer, R.E. Pogson, Spectrochim. Acta, A79 (2011) 1149.

185 [23] R.L. Frost, B.J. Reddy, S.J. Palmer, E.C. Keeffe, Spectrochim. Acta, A78 (2011) 996.

186 [24] J.W. Anthony, R.A. Bideaux, K.W. Bladh, M.C. Nichols, Handbook of Mineralogy
187 Vol.IV. Arsenates, phosphates, vanadates - Mineral Data Publishing, Tucson, Arizona.
188 Mineral data Publishing, Tucson, Arizona, 2000.

189 [25] V.C. Farmer, Mineralogical Society Monograph 4: The Infrared Spectra of Minerals.
190 1974.

191 [26] J. Sejkora, J. Skovira, J. Cejka, J. Plasil, J. Geosc. 54 (2009) 355.

192 [27] H.A. Szymanski, L. Marabella, J. Hoke, J. Harter, Appl. Spectrosc. 22 (1968) 297.

193 [28] S.C.B. Myneni, Rev. Mineral 40 (2000) 113.

194 [29] M.D. Lane, Amer. Min. 92 (2007) 1.

195 [30] P. Keller, Neues Jb. Mineral. Mh. 11 (1971H) 491.

196
197

198 **List of Figures**



206

207

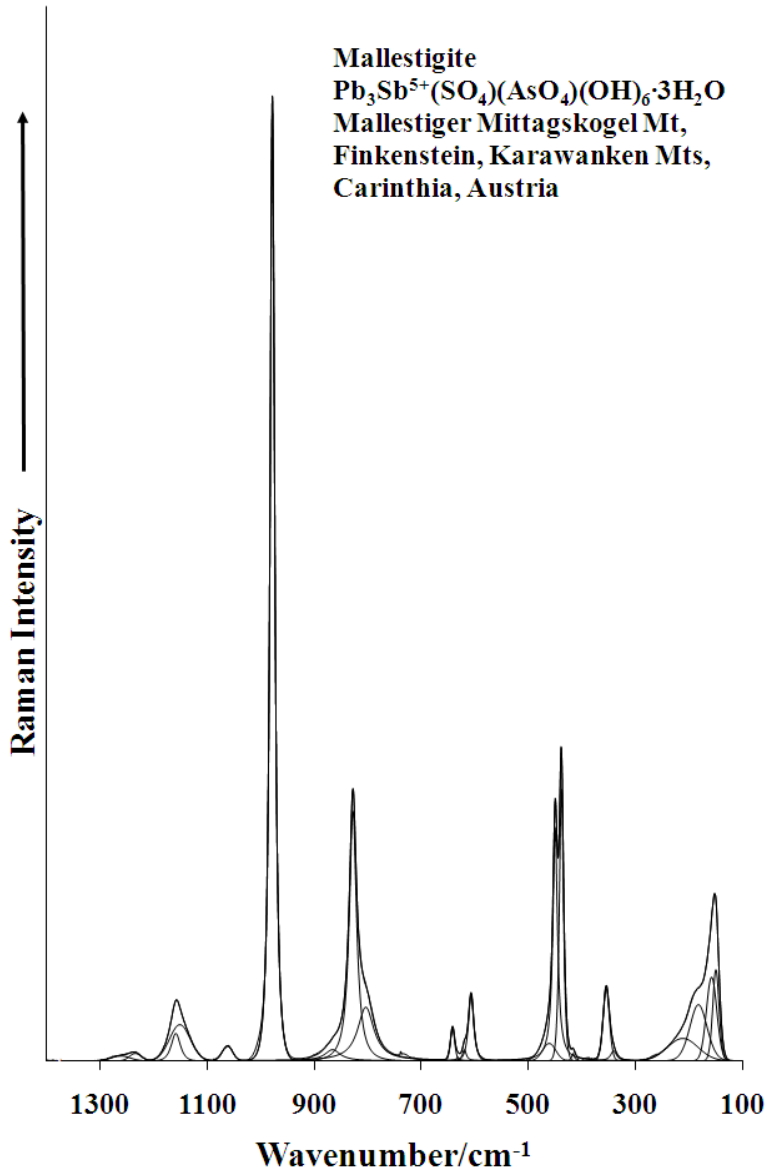


208

209 **Figure 1**

210

211

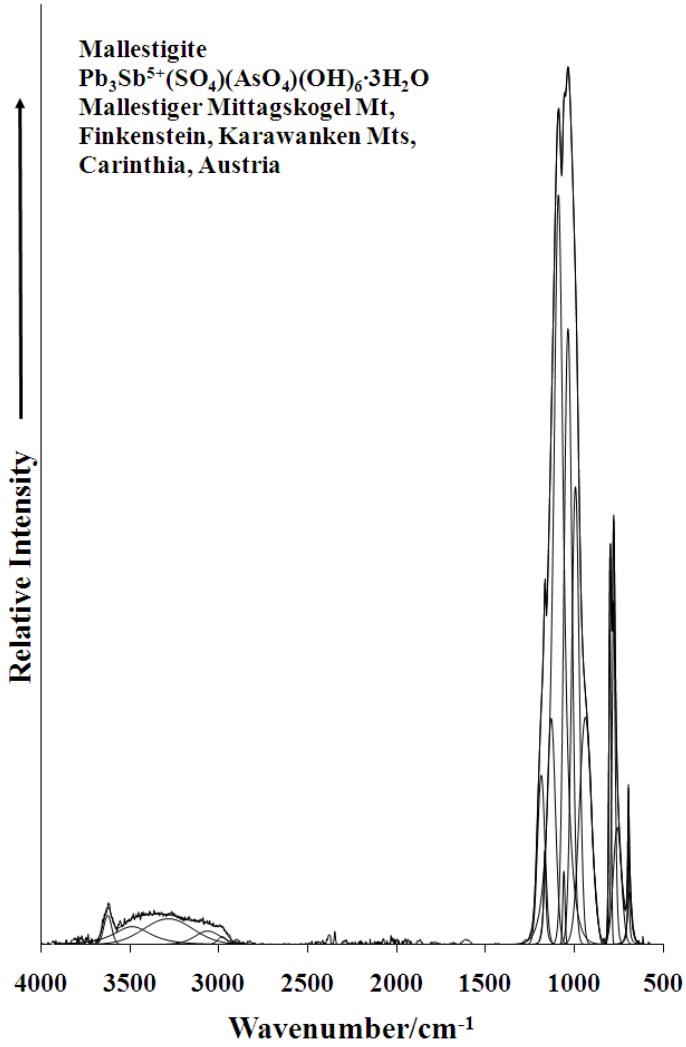
Mallestigite
Pb3Sb5+(SO4)(AsO4)(OH)6·3H2O
Mallestiger Mittagskogel Mt,
Finkenstein, Karawanken Mts,
Carinthia, Austria
Relative Intensity
4000
3500
3000
2500
2000
1500
1000
500
Wavenumber/cm-1

**Figure 2**

219

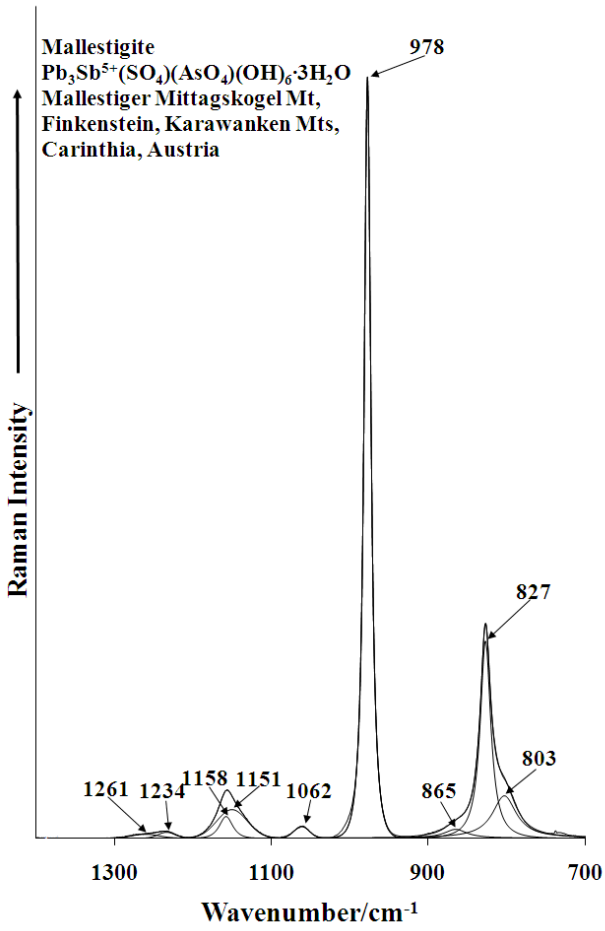


220

221

222 **Figure 3**

223

224

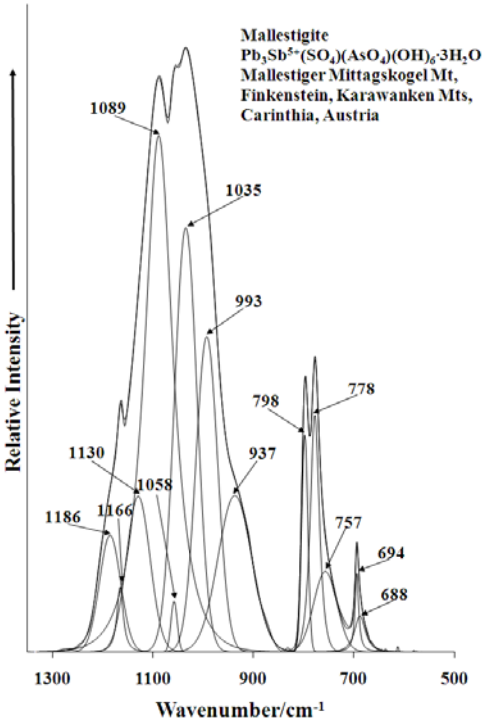


225

226

227 **Figure 4**

228

229

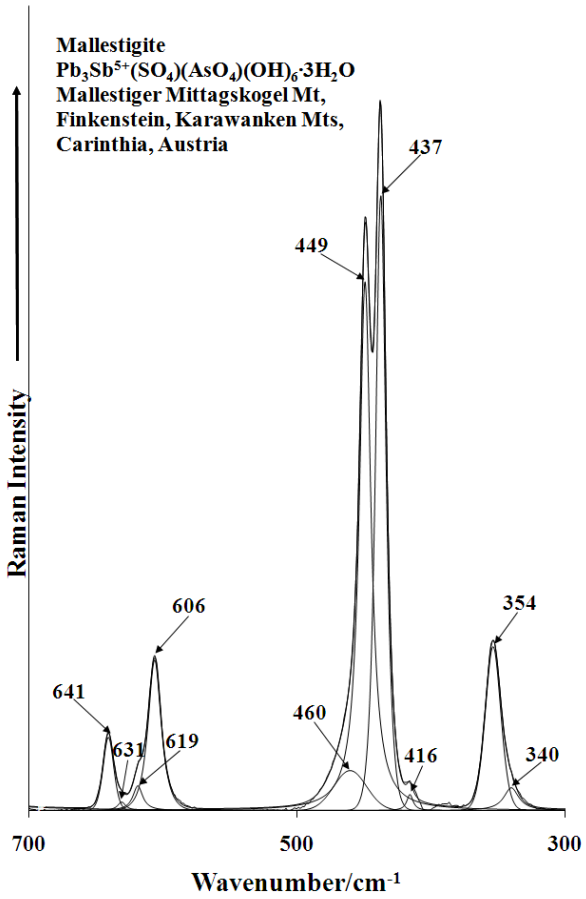


230

231

232 **Figure 5**

233

234

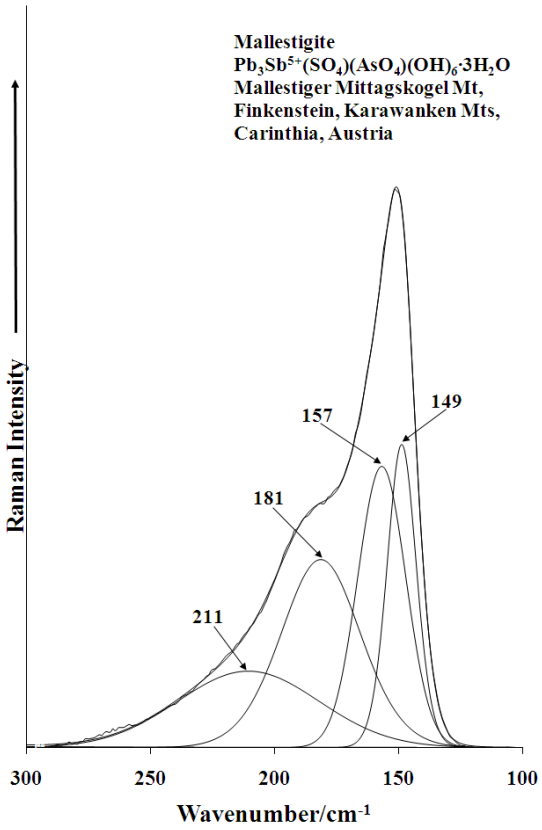


235

236

237 **Figure 6**

238

239

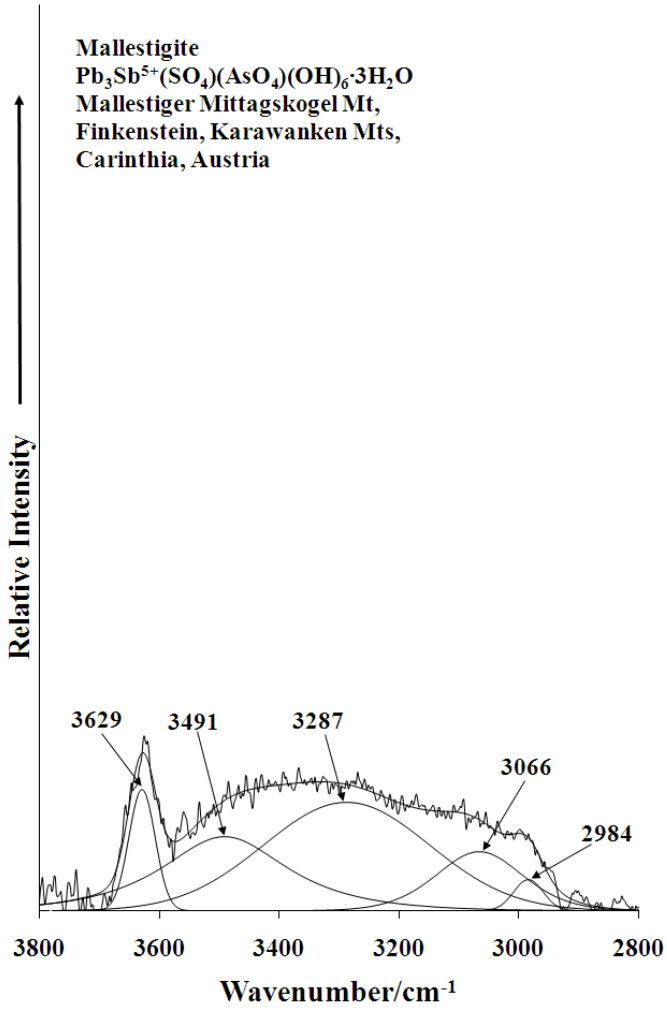


240

241 **Figure 7**

242